ISSN: 1009-1963

中国物理
Chinese Physics

Volume 10 Supplement July 2001
A Publication of the Chinese Physical Society
An International Journal

CHINESE PHYSICAL SOCIETY

CHINESE — GERMAN WORKSHOP

ON

CHARACTERIZATION AND DEVELOPMENT

OF

NANOSYSTEMS

30th October – 2nd November 2000

Chinesisch-Deutsches
Zentrum für
Wissenschaftsförderung

中德科学中心

Sino – German Center for Research Promotion, Beijing

Chinese Physics (First published in 1992)

Published monthly in hard copy by the Chinese Physical Society and online by Institute of Physics Publishing, Dirac House, Temple Back, Bristol BS1 6BE, UK.

Institutional subscription information: 2001 volume
For all countries, except the United States, Canada and Mexico, the subscription rate is £550.00 per annual volume. Single-issue price £45.83. Delivery is by air-speeded mail from the United Kingdom to most overseas countries, and by airfreight and registered mail to subscribers in India.
Orders to:
Order Processing Department, Institute of Physics Publishing, Dirac House, Temple Back, Bristol BS1 6BE, UK

For the United States, Canada and Mexico, the subscription rate is US$1080.00 per annual volume. Delivery is by transatlantic airfreight and onward mailing.
Orders to:
American Institute of Physics Subscriber Services
Suite 1NO1, 2 Huntington Quadrangle, Melville, NY 11747 - 4502, USA

Supported by the National Natural Science Foundation of China, China Association for Science and Technology, and Chinese Academy of Sciences

Editorial Office: Institute of Physics, Chinese Academy of Sciences, P.O. Box 603, Beijing 100080
Tel: (86 - 10) 82649026 or 82649656
Fax: (86 - 10) 82649027, E-mail: wulixb@aphy.iphy.ac.cn

主 办 单 位：中国物理学会
承 办 单 位：中国科学院物理研究所
编　　　辑：《中国物理》编辑部
国 内 发 行：《中国物理》出版发行部
国 外 发 行：Institute of Physics Publishing Ltd
发 行 范 围：公开发行
国 际 统 一 刊 号：ISSN 1009 - 1963
国 内 统 一 刊 号：CN 11 - 4407/O3
编辑部地址：北京 中关村 中国科学院物理研究所内
通 讯 地 址：100080 北京 603 信箱《中国物理》编辑部
电　　　话：(010) 82649026, 82649656
传　　　真：(010) 82649027
E-mail: wulixb@aphy.iphy.ac.cn
http://wulixb.iphy.ac.cn

(Continued on the back of page 205)

Editorial

In this special issue of Chinese Physics manuscripts of lectures and posters are published, which were presented at the Chinese - German workshop on "Characterization and Development of Nanosystems" held at the Sino - German Center for Research Promotion, Beijing, from October 30 to November 2, 2000. The workshop was organized by the Institute of Physics of the Chinese Academy of Sciences and the Institute for Nanotechnology of the Karlsruhe Research Center within the framework of a bilateral cooperation project on fundamentals of nanotechnolgy.

The workshop contributions reflected a broad field of research activities in nanoscience: Apart from seven plenary lectures, 28 special lectures and 17 posters have been presented, dealing with the following subjects: Manipulation and tunneling; nanocrystalline materials; tubes, wires and clusters; organic molecules and biomaterials; growth and fluctuation phenomena as well as structuring, sensoring, and storage on the nanometer scale.

We take the opportunity to express our gratitude to all authors for their contributions to this issue as well as to the reviewers for their efforts to the ensuring the high quality of the published papers. We are grateful to the Editor –in - Chief of Chinese Physics Prof. Wang Nai-yan for the excellent cooperation and the production team for the careful preparation of this issue.

The organizers of the workshop are also grateful to the sponsors, who financed the workshop and enabled the preparation of this special issue, they are: Center of Materials Science, Chinese Academy of Sciences, National Natural Science Foundation of China, Ministry of Science and Technology of China, Chinese Academy of Sciences, Karlsruhe Research Center, International Office of the German Ministry of Research and Education, German Research Society, Sino - German Center for Research Promotion.

Last but not least, we would like to thank all colleagues from the Institute of Physics, the Physics Department of the Peking University, the Sino - German Center, and the Institute for Nanotechnology for their engaged contributions to the success of the workshop and especially also to the supporting program.

Beijing and Karlsruhe, June 2001

Shen Dian-hong
Peter von Blanckenhagen
Editors

Sponsors

Center of Material Science, Chinese Academy of Sciences National Natural Science Foundation of China

Ministry of Science and Technology of China

Chinese Academy of Sciences

Karlsruhe Research Center, Germany

Omicron Vacuumphysik GmbH

International Office of the German Ministry of Research and Education

German Research Society

Sino – German Center for Research Promotion

Venue of the workshop

Sino – German Center for Research Promotion, National Natural Science Foundation of China, Beijing , 83# Shuangqin-lu, Beijing 100085, China

Organizing committee

Shen Dian-hong, Sun Mu and Xie Fang-qing, The State Key Laboratory of Surface Science, Institute of Physics, Chinese Academy of Sciences, P.O. Box 603, Beijing, 100080, China; Phone: +86-10-82649425; Fax: +86-10-82649531; e-mail: dhshen@aphy.iphy.ac.cn

Peter von Blanckenhagen and Wolfram Schommers, Karlsruhe Research Center, Institute for Nanotechnology, D-76021 Karlsruhe, Germany; Phone +49- 7247- 82 3992; Fax: +49- 7247- 82 6368; e-mail: peter.blanckenhagen@ int.fzk.de

(***Continued***)

Instructions to Contributors

Chinese Physics (CP) is an international journal edited and published monthly in English by the Chinese Physical Society (CPS). It is an authoritative, comprehensive academic journal, aiming to reflect creative and innovative achievements in theory and experiment in all fields of physics in China. Each issue contains about 80 printed pages.

The journal accepts manuscripts which have not been published previously nor currently submitted for publication elsewhere. Manuscripts should be sent by registered mail to the CP Editorial Office, P. O. Box 603, Beijing 100080, P. R. China; and a written statement of transfer of copyright to CPS should accompany the act of submitting the manuscript by the author. The publication charges are ¥130/printed page for Chinese authors; for foreign authors it is $30/printed page.

Manuscripts should be submitted in duplicate, and written in concise, legible English, which must be in the **final form** after careful review by the author to eliminate all possible mistakes in content and/or in grammar. Ordinary or standard scientific terms should be used, not an arbitrary translation of the corresponding native or Chinese ones, except those first invented by the author. Abbreviations and symbols should be made according to the conventions approved by IUPAP or International Standards Organization, and the SI system should be used for units of measure throughout the text. No further corrections by authors are permitted, once the manuscript is typeset, or after the final proof has been sent to the author.

Manuscripts should be neatly typed double spaced on only one side of good white paper (of size ~21cm×26cm) with letters not smaller than 10 pt and ample margins (not less than 25mm) on all sides; the length should not be more than 15 pages for a regular paper, and 8 pages for a short note. The items included in the manuscript should be arranged in the following manner: 1) title of the paper; 2) author's name (for Chinese authors, spelled in the Chinese phonetic alphabet followed by the corresponding Chinese characters); 3) author's affiliation (in conventional English, for Chinese authors with the address spelled in Chinese phonetics followed by the corresponding Chinese characters), postcode and name of the country; 4) abstract in English (and for Chinese authors also in Chinese), limited to about 200 words; 5) PACC numbers, four sets at most (authors should refer to those published by "Physics Abstracts"; 6) keywords no more than 4 sets; 7) text; 8) acknowledgements; 9) the supporting organization(s) (and contract number) should be written as a footnote on page 1; 10) references.

Formulas in linear form (e. g. $\exp\,(-1/(x^2+y^2)))$ are preferred, and each should be indicated by a serial number in parentheses placed on the right hand side of the paper. Letters denoting variables in formulas are normally printed in italics, but abbreviations such as sin, log, max etc. and figures are printed in ordinary typeface.

Table(s) should be typed directly at the appropriate location(s) within the text and arranged successively with Arabic numerals.

Figures (including photographs) should be submitted on separate sheets, not included in the text, in a form ready for reproduction, and marked on the back of each sheet with figure number and name of the author in pencil. Drawings should be carefully made using Indian ink on sulfate paper, and the lines must be smooth, clean and uniform, with notations clearly made in pencil. The size of the figures can be between 14cm×20cm and 7cm×10cm, and **in the text the positions where figures may be inserted should be marked by boxes of a suitable size with the figure captions typed under them.** Photographs should be selected with good contrast and clearly distinguishable details.

Footnotes, other than those which refer to the title heading, should be numbered successively and placed at the foot of the page to which they refer (not at the end of the paper).

References to the literature should be listed at the end of the manuscript, and numbered consecutively with square brackets enclosing the number, in the sequence they appear. For **journal articles** the following information should be provided: names of all authors, year of publication, name of the journal (use conventional abbreviations), volume and page, for example:

[1] Meyer F 1974 *Phys. Rev.* B **9** 3622

Reference to **books** should include name(s) of author(s), year of publication, full title, edition (omitted for the first edition), place of publisher, publication and page or chapter, for example:

[2] Bloembergen N 1965 *Nonlinear Optics* (New York: Benjamin) p 12

The format of a published paper in CP can be found in a recent issue.

The author should reserve an identical original manuscript for reference. A manuscript can be sent to referees only when it meets the requirements mentioned above; otherwise, it will be returned to the author for modification. If the manuscript cannot be accepted, it will be sent back to the author. An electronic version of the manuscript will be requested after acceptance of the paper, but floppy disks will not be returned to the author. Once the article is published in this journal, 30 reprints will be sent to the author free of charge.

Structuring, sensoring and storage

Recent developments

Vol 10 Suppl., July 2001
1009-1963/2001/10(Suppl.)/00S1-03

Chinese Physics

SINGLE-ELECTRON TRANSISTORS FOR FUTURE APPLICATIONS*

WANG TAI-HONG(王太宏), LI HONG-WEI(李宏伟) and ZHOU JUN-MING(周均铭)

Institute of Physics, Chinese Academy of Sciences, Beijing 100080, *China*

(Received 1 January 2001; revised manuscript received 6 February 2001)

Single electron transistors with wire channels are fabricated by a nanoelectrode-pair technique. Their characteristics strongly depend on the channel widths and the voltages on the in-plane gates. A few dips in the Coulomb blockade oscillations were observed at the less positive gate voltages for a device with a 70nm-wide wire due to Coulomb blockade between the coupled dots. By applying negative voltages to the in-plane gates, the oscillations became periodic, which indicated the formation of a single dot in the conducting channel. These gates facilitate fabricating single-electron transistors with single dot structures, which have potential applications on its integration.

Keywords: single-electron tunneling, Coulomb blockade, quantum dots
PACC: 7280E, 7335C, 7340G

With the recent rapid progress of fabrication techniques for nanostructures, many types of single-electron transistors (SET) have been fabricated. From the engineering viewpoint, single-electron transistors with wire channels[1–7] have a larger chance to be used to construct next-generation electronics with new system architectures. These transistors are not only suitable for their integration but also have potential applications in investigating quantum effects. Efforts have been paid to raise their working temperatures. The operation at room temperature for such kinds of devices has also been reported.[2] However, some of these devices have shown complicated behaviors because of the formation of multiple-dots in the wire channels. The realization of the high-temperature operation for these devices is mainly dependent on the channel width. As the channel width is decreased, the fluctuation of the geometric width becomes more serious. This leads to the formation of multiple-dots. Therefore, it is very important to develop techniques which can be used to realize one single dot in the narrow channels. We have combined the in-plane gate technique and the split-gate technique and developed them into a nanoelectrode-pair technique. By using this technique, we fabricated Si single-electron transistors with in-plane point contact metal (IPPCM) gates by using a self-aligned process. Point contacts were formed by etching a constriction with a designed length of 100nm and a width of 70nm. The effective width of the conducting area can be modified by biasing the IPPCM gates. The pattern was defined by photolithography and mesa-etching.

Figure 1 shows the schematic view of the single-electron transistors with IPPCM gates. A (001) oriented, p-type silicon-on-insulator (SOI) substrate prepared by the separation by implanted oxygen (SIMOX) technique was employed. The silicon single crystal layer was thinned by repeated thermal oxidation and HF etching of the oxide to 70nm. A point contact channel was formed in the Si layer between source and drain electrodes by photolithography and electron-cyclotron-resonance (ECR) plasma etching. Then the wafer was subjected to thermal oxidation in dry oxygen ambient. By using a self-aligned process, IPPCM gates were deposited. This was realized by rotating the wafer to expose both sides of the channel during evaporation. A layer of silicon dioxide with the thickness of 80nm was deposited and finally a top metal gate was formed. The oxide layer serves to insulate the IPPCM gates and the top gate. Applying positive voltages to the top gate leads to the formation of two-dimensional electron gases (2DEGs) at the inversion layer and controls the electrostatic potential of the SET island. Here we report on transport beharior of one device with 70nm-wide channel.

*Project supported by the National Natural Science Foundation of China (Grant Nos. 69925410 and 19904015).

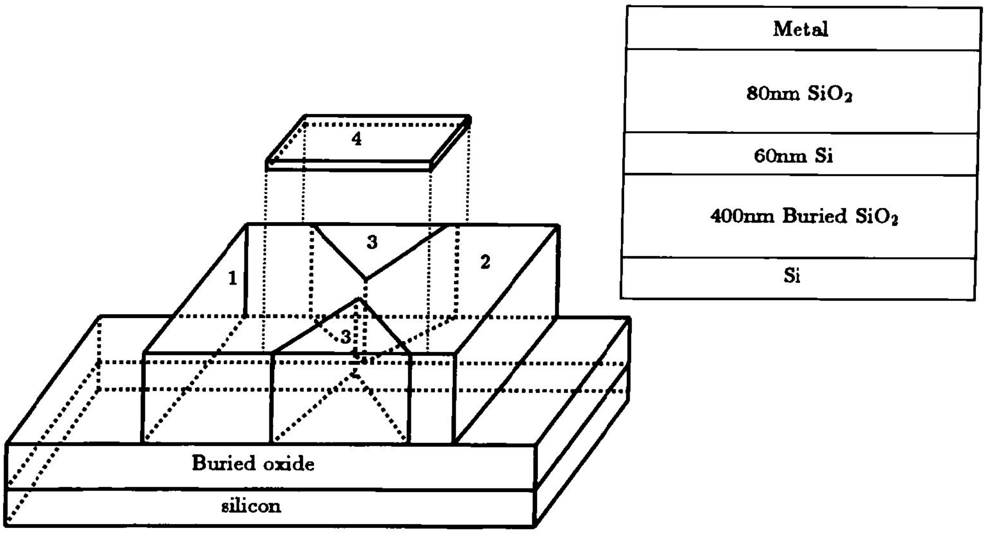

Fig.1. A schematic illustration of the fabricated device. The source and the drain are indicated by 1 and 2, the in-plane gates by 3, and the top gate by 4.

Figure 2 shows the drain current I_2 versus the top gate voltage V_4 characteristic of the device with 70nm-wide channel. The source is grounded. With scanning V_4, I_d oscillates and decreases significantly at V_4 <3.5V. Above V_4=3.5V, both the amplitude of the oscillations and the minimum of the current change a little. In the range of 0.22V< V_4 <3.5V, I_d shows peaks at 2.16, 1.89, 1.36, 1.12, and 0.53V, and also exhibits dips at 2.26, 1.97, 1.41, and 0.90V. The shape of these three peaks is irregular and similar to that of the peaks above 3.5V. The irregular shape is typical characteristic of the Coulomb blockade oscillations (CBOs) through coupled dots.[7−9] Therefore, it can be inferred that a number of dots are formed at the constriction.

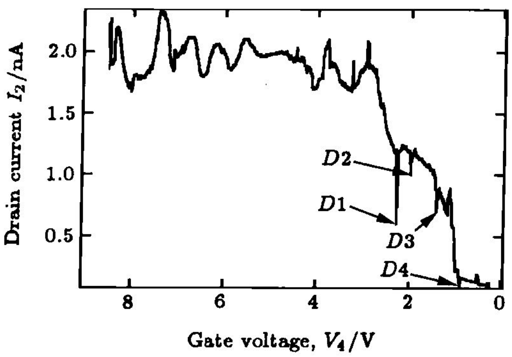

Fig.2. I_2-V_4 characteristic of the device with 70nm-wide channel at V_2=1mV, V_3=0mV, and T=4.2K.

It could be easily understood by simply assuming that five dots be formed, as shown in Fig.3. The dips, which are indicated by $D1$, $D2$, $D3$, and $D4$ in Fig.2 arise from the stochastic Coulomb blockade within the multiple-dot structure.[7−9] Decreasing V_4 reduces the electron density in the inversion layer. Below some critical density, electrons localize in the potential minimum within the channel. So quantum dots are formed at the constriction. We argue that dots are formed even in the range 9V> V_4 >3.5V from the observation of both the irregular shape and their Coulomb staircases.

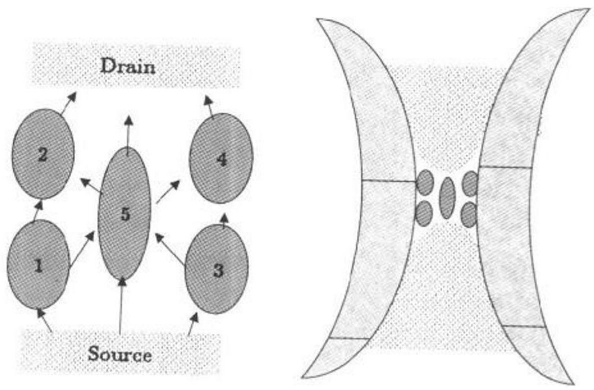

Fig.3. The shape of the channel and formation of the dots. The channel has a length of about 100nm and a width of 70nm.

Considering the shape of the channel, we assume that two dots be formed at each side of the channel and one dot at the center. This is reasonable because the fluctuation of the potential at the edge of the channel is more serious than that at the center of the channel. Transport through the channel is controlled by charging and discharging of all these five dots. For a special arrangement of the charge within the five dots, either Dot-1, Dot-2, and Dot-3 or Dot-5, Dot-2, and Dot-4 are in the Coulomb blockade regime. For such two cases, the channel was blockaded and no electrons can flow through the channel. These gives rise to a sharp drop in the drain current.[6,10,11] The drain current at the four dips in Fig.2 is not zero and this could be partly caused by cotunneling.

Applying negative voltages on the in-plane gates V_3 squeezes the channel and depletes Dot-1, Dot-2, Dot-3, and Dot-4. The electrostatic potential of the four dots is raised so that all the electrons in these four dots are moved out and no other electrons can tunnel into these dots. So the charging and discharging disappear in the four dots. In this case, only Dot-5 controls the current flow through the channel and this leads to the observation of the CBOs with a period of 0.64 V in Fig.4.

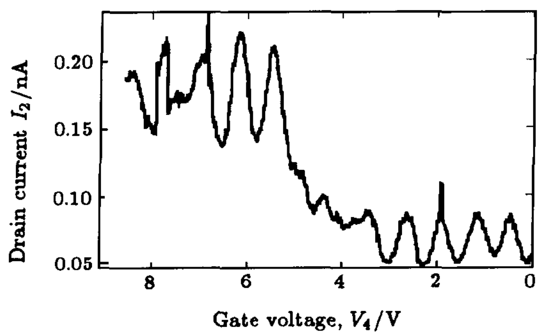

Fig.4. Coulomb blockade oscillations of the devices with 70nm-wide channel at V_2=1mV, V_3=–116mV, and T=4.2K.

Formation of dots could arise from (1) the thickness fluctuations of the SOI layer, (2) the fluctuation of the channel width, (3) pattern dependent oxidation, (4) strain by etching and oxidation, (5) localized states and (6) Si nanoparticles at the interface between the SOI layer and the buried oxide layer. The narrow channel in our case is a point contact wire and the period of the thickness fluctuations should be much larger than its wire length. This rules out the thickness fluctuations for the formation of the dots. Ishikuro *et al.*[2] reported formation of the dots resulting from the fluctuation of the channel width. This contradicts our results on formation of multiple-dots for the devices with wide channels. We also checked the devices without thermal oxidation and found that CBOs could not be observed in these devices. So the considerable band gap shrinkage[12] from the oxidation induced compressive strain probably accounts for the formation of the dots in our devices.

In summary, we investigated a Si single-electron transistor with in-plane point metal gates. The device with 70nm-wide channel exhibited dips in the $I_2 - V_4$ characteristic, which were attributed to stochastic Coulomb blockade within the multiple-dot structure. By applying negative voltages on the in-plane gates, the device showed clear periodic CBOs. These indicate that the in-plane point gates can be used to realize single-electron transistors with single dot structures.

References

[1] Nakazato K, Thornton T J, White J and Ahmed H 1992 *Appl. Phys. Lett.* **61** 3145

[2] Ishikuro H and Hiramoto T 1999 *Appl. Phys. Lett.* **74** 1126

[3] Smith R A and Ahmed H 1997 *Appl. Phys. Lett.* **71** 3838

[4] Kasai S, Jinushi K, Tomozawa H and Hasegawa H 1997 *Jpn. J. Appl. Phys.* Part 1 **36** 1678

[5] Fu Y, Wang T H and Willander M 2001 *J. Appl. Phys.* **89** 1759

[6] Wang T H and Aoyagi Y 2001 *Appl. Phys. Lett.* **78** 634

[7] Wang T H and Tarucha S 1997 *Appl. Phys. Lett.* **71** 2499

[8] Kemerink M and Molenkamp L W 1994 *Appl. Phys. Lett.* **65** 1012

[9] Ruzin I M, Chandrasekhar V, Levin E I and Glazman L I 1996 *Phys. Rev.* B **45** 13469

[10] Hofmann F, Heizel T, Wharam D A, Kottaus J P, Bohm G, Klein W, Trankle G and Weimann G 1995 *Phys. Rev.* B **51** 13872

[11] Van der Vaart N C, Kouwenhoven L P, van Steveninck M P De Ruyer, Nazarov Y V, Harmans C J P M and Foxon C T 1997 *Phys. Rev.* B **55** 9746

[12] Shiraishi K, Nagase M, Horiguchi S, Kageshima H, Uematsu M, Takahashi Y and Murase K 2000 *Physica* E **7** 337

Vol 10 Suppl., July 2001
1009-1963/2001/10(Suppl.)/00S4-06

Chinese Physics

RESONANT ANDREEV REFLECTION IN HYBRID SUPERCONDUCTING-NORMAL NANOSTRUTURES*

LIN TSUNG-HAN(林宗涵)

State Key Laboratory for Mesoscopic Physics Department of Physics, Peking University, Beijing 100871, *China*

(Received 11 February 2001)

After a brief description of hybrid superconducting-normal nanostructures and a brief introduction of the Andreev reflection, we present a theoretical investigation of the electron tunneling through a normal-metal/quantum-dot/superconductor (N-QD-S) system where multiple discrete levels of the QD is considered. By using the nonequilibrium-Green- function (NGF) method, the current I is obtained and studied in detail. We find that the Andreev tunneling shows clear resonant behavior, as obtained in previous works. Moreover, the current I versus the gate voltage V_g exhibits different kinds of peaks, depending on the bias voltage, the level-spacing of the QD, and the energy gap of the superconducting electrode. Besides, in I-V characteristics extra peaks superimposed on the conventional current plateaus emerge, which stem from the resonant Andreev reflections.

Keywords: transport properties, tunneling phenomena
PACC: 7430F, 7450

I. INTRODUCTION

Since early 1990s, the tremendous development of the nanofabrication technology has made it possible for manufacturing various hybrid superconducting-normal (S-N) structures, leading to the emergence of a very active research field. As a review of the achievements of early 1990s, the International Symposium on "Mesoscopic Superconductivity " was held in Karlsruhe, Germeny in 1994.[1]

What is interesting in hybrid S-N nanostrutures? It is well known that the essential fearture of mesoscopics is the phase coherence of carriers, electrons or holes; while the superconductivity is a macroscopic quantum condensate with the coherence of Cooper pairs. How these two coherence effects couple with each other? The key mechanism is Andreev reflection, which causes the interplay of the above two kinds of coherences possible, and makes this new field of the condensed matter physics a very fruitful one. It was proposed by Andreev [2] that an electron is reflected from N-S interface in a peculiar way. Because of the energy gap of the superconductor, an electron incoming from normal metal with an energy ϵ below the gap is forbidden to enter the superconductor. However, the incoming electron with the energy ϵ and up-spin may pick up an electron with the energy $-\epsilon$ and down-spin, both entering into the superconductor and forming a Cooper pair; meanwhile a hole with a up-spin is left and going back to the normal metal. Although Andreev reflection is a second order process, it dominates for the clean N-S interface at low temperatures and small bias, since the conventional first order processes are forbidden.[3,4]

II. MAIN PROPERTIES OF ANDREEV REFLECTION

The basic properties of Andreev reflection (AR) are: (1) Retro-reflection: the group velocities of the incident electron and Andreev reflected hole are in opposite directions (perfect only for the electron incoming at the Fermi level). (2) AR is a two-particle process, by which the normal current in N is converted into supercurrent in S. (3) AR is a phase coherent process: the Andreev reflected hole(electron) carries phase information both from the incident elctron(hole) and from the the superconductor.[3,4]

Because the combination of mesoscopics and superconductivity, a number of novel and interesting effects appear, including the quantization of the maximum supercurrent of the superconducting quantum point contacts (SQPC); the enhanced conductance oscillations in Aharonov-Bohm ring with superconducting "mirrors"; the enhanced shot noise in N-S junctions; the AR bound states in SNS structures; the even-odd asymmetry in N-SQD-N and S-SQD-S sys-

*Project supported by the Visiting Scholar Foundation of Key State Laboratory for Mesoscopic Physics in Peking University and by National Natural Science Foundation of China (Grant No.10074001).

tems; the supercurrent control and reverse in SNS; the nonequilibrium and proximity effects in systems with ferromagnetic elements; the hybrid systems with carbon nanotube; etc.[1,3-9]

Works we have done for mesoscopic hybrid S-N structures include: (1) For the electron transport through a mesoscopic hybrid multiterminal resonant-tunneling system which contains a normal central region coupled to multiple superconducting leads, a general expression of the current is derived. This formula can be used to describe the case with time-dependent external fields applied to any parts of the system, arbitrarily finite voltages, and any kinds of interactions in the central region;[10] (2) Resonant Andreev reflection in a N-QD-S system;[11] (3) Photon-assisted Andreev tunneling through a mesoscopic system;[12] (4) Control of the supercurrent in a four-terminal Josephson junction;[13] and some others.

Here we only present our theoretical investigation for the electron tunneling through a N-QD-S structure, a normal quantum-dot connected to two leads, one is a normal metal and the other is a superconductor. Different from Refs.[14] and [15] where only a single level of the QD has been considered, here we assume that the QD has discrete multiple levels, but the intra-dot Coulomb interactions will be neglected for simplicity. Using the nonequilibrium-Green-function(NGF) method, the current formula has been derived. The dependence of the current I upon the gate-voltage, the bias voltage, the level-spacing of the QD, and the energy gap of the superconducting electrode have also been studied in detail.[11,12]

III. MODEL AND FORMULATION

We assume that the system under consideration is described by the following Hamiltonian[16,17]

$$H(\tau) = H_{\mathrm{L}} + H_{\mathrm{R}} + H_{\mathrm{dot}} + H_{\mathrm{T}}(\tau), \qquad (1)$$

where

$$\begin{aligned} H_{\mathrm{L}} =& \sum_{k,\sigma}(\epsilon^0_{\mathrm{L},k} - ev_{\mathrm{L}})a^\dagger_{\mathrm{L},k\sigma}a_{\mathrm{L},k\sigma} \\ H_{\mathrm{R}} =& \sum_{p,\sigma}\epsilon^0_{\mathrm{R},p}a^\dagger_{\mathrm{R},p\sigma}a_{\mathrm{R},p\sigma} \\ &+ \sum_{p}\left[\Delta^* a_{\mathrm{R},p\downarrow}a_{\mathrm{R},-p\uparrow} + \Delta a^\dagger_{\mathrm{R},-p\uparrow}a^\dagger_{\mathrm{R},p\downarrow}\right] \\ H_{\mathrm{dot}} =& \sum_{i,\sigma}(\epsilon^0_i - eV_{\mathrm{g}})c^\dagger_{i\sigma}c_{i\sigma}, \qquad (2) \\ H_{\mathrm{T}} =& \sum_{k,\sigma,i}\left[t_{\mathrm{L}}a^\dagger_{\mathrm{L},k\sigma}c_{i\sigma} + t^*_{\mathrm{L}}c^\dagger_{i\sigma}a_{\mathrm{L},k\sigma}\right] \\ &+ \sum_{p,\sigma,i}\left[t_{\mathrm{R}}e^{iev_{\mathrm{R}}\tau}a^\dagger_{\mathrm{R},p\sigma}c_{i\sigma} + t^*_{\mathrm{R}}e^{-iev_{\mathrm{R}}\tau}c^\dagger_{i\sigma}a_{\mathrm{R},p\sigma}\right]. \end{aligned}$$

where H_{L} describes the noninteracting electrons in the left normal-metal lead, $a^\dagger_{\mathrm{L},k\sigma}$ ($a_{\mathrm{L},k\sigma}$) are the creation (annihilation) operators of the electron in the left lead, and v_{L} is the voltage of the left lead. H_{R} describes the right superconducting lead with the energy gap Δ. H_{dot} is the Hamiltonian of the quantum dot with multiple discrete energy levels, characterized by the index i and spin σ. For simplicity, the intra-dot electron-electron Coulomb interaction has been neglected. V_{g} is the gate voltage which controls the energy levels in the dot. H_{T} denotes the tunneling part of the Hamiltonian, and t_v ($v = \mathrm{L}, \mathrm{R}$) is the hopping matrix and is assumed to be independent of the state k of the leads and the dot-state (i,σ) for simplicity. In order to obtain the Hamiltonian (1) and (2), we have performed a unitary transformation similar to Ref.[16], so that the voltage of the right lead, v_{R}, appears as a phase factor in the hopping elements.

Since the current is conserved, it is enough to calculate the current from the left lead to the QD. From the evolution of the total number operator of the electrons in the left lead, $N_{\mathrm{L}} = \sum_{k,\sigma} a^\dagger_{\mathrm{L},k\sigma}a_{\mathrm{L},k\sigma}$:[18,19]

$$\begin{aligned} I(\tau) =& -e < \dot{N}_{\mathrm{L}}(\tau) > \\ =& \frac{ie}{\hbar} < [N_{\mathrm{L}}, H] > \\ =& \frac{2e}{\hbar}\mathrm{Re}\sum_{k,i,\sigma} t_{\mathrm{L}} \ll c_{i\sigma}(\tau)|a^\dagger_{\mathrm{L},k\sigma}(\tau)\gg^<, \qquad (3) \end{aligned}$$

where the Green function $\ll A(\tau)|B(\tau')\gg^<$ is defined as: $\ll A(\tau)|B(\tau')\gg^< \equiv i < B(\tau')A(\tau) >$. With the help of Dyson's equation, using the exact Green functions of the electron in the left lead (normal-metal) without the coupling between the dot and the lead, taking a replacement of the sum over k by an integral over energy with the help of the density of states in the left lead, and introducing the linewidth function $\Gamma_{\mathrm{L}}(\omega) = 2\pi|t_{\mathrm{L}}|^2\rho_{\mathrm{L}}(\omega)$, then Eq.(3) becomes to

$$\begin{aligned} I(\tau) =& -\frac{4e}{\hbar}\mathrm{Im}\int\frac{d\omega}{2\pi}\Gamma_{\mathrm{L}}\int_{-\infty}^{\tau}d\tau' e^{i(\omega-ev_{\mathrm{L}})(\tau-\tau')} \\ &\cdot\sum_{i,j}\Big[\ll c_{i\uparrow}(\tau)|c^\dagger_{j\uparrow}(\tau')\gg^r f_{\mathrm{L}}(\omega) \\ &+ \ll c_{i\uparrow}(\tau)|c^\dagger_{j\uparrow}(\tau')\gg^<\Big] \\ \equiv& -\frac{4e}{\hbar}\mathrm{Im}\int\frac{d\omega}{2\pi}\Gamma_{\mathrm{L}}\int_{-\infty}^{\tau}d\tau' e^{i(\omega-ev_{\mathrm{L}})(\tau-\tau')} \\ &\cdot\left[\boldsymbol{G}^r(\tau,\tau')f_{\mathrm{L}}(\omega) + \boldsymbol{G}^<(\tau,\tau')\right]_{11}, \qquad (4) \end{aligned}$$

where $f_{\rm L}(x)=[\exp(x/k_{\rm B}\mathcal{T})+1]^{-1}$ is the Fermi distribution function with $\mathcal{T}$ the temperature, and we have introduced the Nambu representation (2×2 matrix) of the Green functions $\boldsymbol{G}^r(\tau,\tau')$ and $\boldsymbol{G}^<(\tau,\tau')$:[16,20]

$$\boldsymbol{G}^{r,a}(\tau,\tau')\equiv\mp i\theta(\pm\tau\mp\tau')\sum_{i,j}\begin{pmatrix} <\{c_{i\uparrow}(\tau),c^\dagger_{j\uparrow}(\tau')\}> & <\{c_{i\uparrow}(\tau),c_{j\downarrow}(\tau')\}> \\ <\{c^\dagger_{i\downarrow}(\tau),c^\dagger_{j\uparrow}(\tau')\}> & <\{c^\dagger_{i\downarrow}(\tau),c_{j\downarrow}(\tau')\}> \end{pmatrix}, \tag{5}$$

$$\boldsymbol{G}^<(\tau,\tau')=i\sum_{i,j}\begin{pmatrix} <c^\dagger_{j\uparrow}(\tau')c_{i\uparrow}(\tau)> & <c_{j\downarrow}(\tau')c_{i\uparrow}(\tau)> \\ <c^\dagger_{j\uparrow}(\tau')c^\dagger_{i\downarrow}(\tau)> & <c_{j\downarrow}(\tau')c^\dagger_{i\downarrow}(\tau)> \end{pmatrix}. \tag{6}$$

After a tedious calculation (details see Refs.[11] and [12]), we finally obtain the following current formula:

$$I=I_A+I_1\ ,$$

with

$$I_{\rm A}=\frac{2e\Gamma_{\rm L}^2}{\hbar}\int\frac{{\rm d}\omega}{2\pi}\left|\tilde{G}^r_{12}\right|^2[f_{\rm L}(\omega+ev_{\rm L}-ev_{\rm R}) - f_{\rm L}(\omega-ev_{\rm L}+ev_{\rm R})], \tag{7}$$

$$I_1=\frac{2e\Gamma_{\rm L}\Gamma_{\rm R}}{\hbar}\int\frac{{\rm d}\omega}{2\pi}\tilde{\rho}_{\rm R}(\omega)\left[\left|\tilde{G}^r_{11}\right|^2+\left|\tilde{G}^r_{12}\right|^2 - \frac{2\Delta}{|\omega|}{\rm Re}\left[\tilde{G}^r_{11}(\omega)(\tilde{G}^r_{12}(\omega))^*\right]\right] \cdot[f_{\rm L}(\omega+ev_{\rm L}-ev_{\rm R})-f_{\rm R}(\omega)]. \tag{8}$$

The formulas of the current, Eqs.(7) and (8), are the central results of this paper. The current I_A represents the contribution from the Andreev reflection. The current I_1 consists of three different processes:[16] (1) The conventional electron tunneling through the system, i.e., the term $\Gamma_{\rm L}\Gamma_{\rm R}\tilde{\rho}_{\rm R}|\tilde{G}^r_{11}(\omega)|^2$; (2) An electron incident from the left lead will convert into a holelike in the right superconducting lead, i.e., the term $\Gamma_{\rm L}\Gamma_{\rm R}\tilde{\rho}_{\rm R}|\tilde{G}^r_{12}(\omega)|^2$, corresponding to a "branch crossing" process in the BTK's theory;[21] (3) An electron (or a hole) incident from the left lead tunnels into the right superconducting lead, picks up a quasi-particle (or a quasi-hole) in the superconductor and creates (or annihilates) a Cooper pair, i.e., the term $-\Gamma_{\rm L}\Gamma_{\rm R}\tilde{\rho}_{\rm R}\frac{2\Delta}{|\omega|}{\rm Re}[\tilde{G}^r_{11}\tilde{G}^{r*}_{12}]$. At zero temperature, if $|eV|<\Delta$ one has $I_1=0$, i.e., only the Andreev reflection process contributes to the current. However, when $|eV|>\Delta$, all of the processes mentioned above make the contributions to the current.

IV. DIFFERENT SERIES OF RESONANT ANDREEV REFLECTION PEAKS

On the basis of the current formulas, Eqs.(7), and (8), we investigate the properties of the current I versus the gate voltage $V_{\rm g}$. Unlike the system of N-QD-N in which the current I versus the gate voltage $V_{\rm g}$ at small bias V exhibits a single series of equally spaced resonance peaks. Now with one of the leads replaced by a superconducting lead, the situation becomes more complicated. In the following we shall discuss in detail two different cases for $eV<\Delta$ and $eV>\Delta$. We set (1) the temperature $\mathcal{T}=0$, (2) the voltage of the right leads $v_{\rm R}=0$ due to the gauge invariance, and carry out all calculations in units of $\hbar=e=1$.

A. The case with $V<\Delta$

In this case only the Andreev reflection current I_A exists. Figure 1 presents I vs $V_{\rm g}$ at different bias. In numerical studies, we have assumed that the QD has 10 discrete levels with equal level-spacing. These levels move downward as $V_{\rm g}$ increases. At small bias, I vs $V_{\rm g}$ exhibits a single series of peaks with equal spacing (marked with "A" in Fig.1(a)). Notice that these resonance peaks are not due to the conventional resonant tunneling, because the conventional tunneling is completely forbidden for $V<\Delta$. Insteadly, these peaks come from the Andreev reflections. When the energy of a state-i of the QD is lined up with the chemical potential of the right superconducting lead, $\mu_{\rm R}$ ($\mu_{\rm R}=-v_{\rm R}$ is set to be zero), then an electron incident from the left lead with the energy $\epsilon=\mu_{\rm R}$ can tunnel into the state-i of the QD, leading to a hole propagating back to the state-i in the QD and the creation of a Cooper pair in the right superconducting lead because of Andreev reflection (see Fig.2(a)). As a result, a current peak emerges in the $I-V_{\rm g}$ curve. Notice that in this Andreev reflection process the incident electron and the reflected hole go through the same state-i of the QD. If the energy level is not lined up with $\mu_{\rm R}$, the Andreev reflection will be very weak, corresponding to a very small Andreev reflection current I_A.

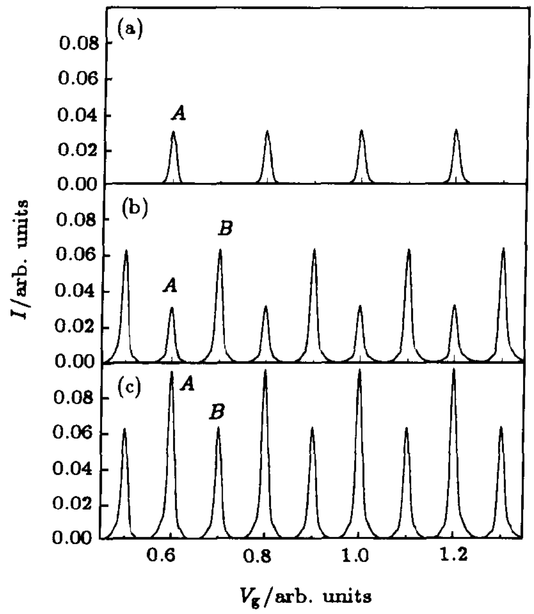

Fig.1. The current I vs the gate voltage V_g for $V < \Delta$. The QD has 10 states with equal level-spacing, $\Delta\epsilon = 0.2$; and $\epsilon_0 = 0$ at $V_g = 0$. Other parameters are chosen as $\Gamma_L = \Gamma_R = 0.01$, $\Delta = 1$. (a), (b), and (c) corresponding to three different bias: $V = 0.02$, 0.15, and 0.25, respectively.

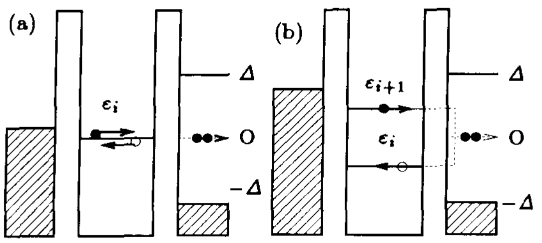

Fig.2. A Schematic diagram for the Andreev reflections: (a) the Andreev reflection through the state-i itself; (b) the Andreev reflection through two states, the state-i and state-$(i+1)$.

Gradually increasing the bias V, the basic feature of I–V_g does not change much, as long as $V < \Delta\epsilon/2$, where $\Delta\epsilon$ is the level-spacing of the QD. Hence the corresponding differential conductance dI/dV is almost zero for $V < \Delta\epsilon/2$. However, when V is greater than $\Delta\epsilon/2$, a series of extra peaks emerges in the I–V_g curve (marked with "B" in Fig.1(b)). The B-type peaks are located in the middle of the A-type peaks with the same peak spacing as that of the A-type peaks, but have much larger amplitudes than that of the A-type peaks (approximately doubled).

The B-type peaks are originated from the following Andreev reflection. For a certain gate voltage V_g, two neighboring states of the QD, say ϵ_i and ϵ_{i+1}, satisfy two conditions: the chemical potential of the right superconducting lead, μ_R, is located in the middle of the two levels; while both of these two levels are below the chemical potential of the left lead, $\mu_L(\mu_L = -v_L)$. So an electron incident with energy $\epsilon = \epsilon_{i+1}$ (or ϵ_i) tunnels from the left lead through the left barrier into the QD's state-$(i+1)$ (or state-i), then Andreev reflected at the right barrier as a hole back to the QD's state-i (or state-$(i+1)$), with a Cooper pair created in the superconductor in the meantime(see Fig.2(b)). Notice that in the B-type Andreev reflection both state-$(i+1)$ and state-i contribute to the current, while the A-type Andreev reflection only involves a single state, so B-type peak has approximately twice the amplitude as that of A-type peak. If $V < \Delta\epsilon/2$, the B-type Andreev reflection can not happen at zero temperature.

When V is less than $\Delta\epsilon$ the amplitude of the A-type peak is smaller than that of the B-type peak. As the bias V is larger than $\Delta\epsilon$ (within the energy range of Γ), the amplitude of the A-type peak becomes larger than that of B-type peak and eventually reaches a height three times it original value (see Fig.1(c)). The positions of A-type peaks do not change. In fact, for a certain gate voltage V_g, a QD's state-i will line up with the chemical potential μ_R, so the Andreev reflection through the state-i itself replaces the original A-type peak. Meanwhile, not only the state-$(i+1)$ and the state-$(i-1)$ are just at $\Delta\epsilon$ and $-\Delta\epsilon$, respectively, both of them are below the left chemical potential μ_L as well, due to the condition $V > \Delta\epsilon$. So the Andreev reflection can also occur through the state-$(i+1)$ and state-$(i-1)$. Now three states $(i-1)$, i, and $(i+1)$ contribute to the A-type peaks, resulting a much higher peak.

In the above numerical calculation, we have assumed that the energy levels in the dot are equal-spacing. If the level-spacing are unequal, the results will be more complicated. Generally, the interval between peaks of each type becomes different from peak to peak. Here we consider a special case of the quantum dot with 10 energy levels and the level-spacig as: $\Delta\epsilon_i = 0.17$ for even i, $\Delta\epsilon_i = 0.23$ for odd i, and $\epsilon_0 = 0$ at $V_g = 0$ ($\Delta\epsilon_i \equiv \epsilon_{i+1} - \epsilon_i$). Figure 3 shows the case of $V > \Delta\epsilon_i$. In contrast to the equal-spacing case (compare to Fig.1(c)), the original A-type peaks are splitted into two peaks (marked with "A_1" and "A_2" in Fig.3). For the unequal level-spacing case, the two peaks from above mentioned two kinds of Andreev reflections no longer overlap completely. So one sees a series of splitted two-peak resonances.

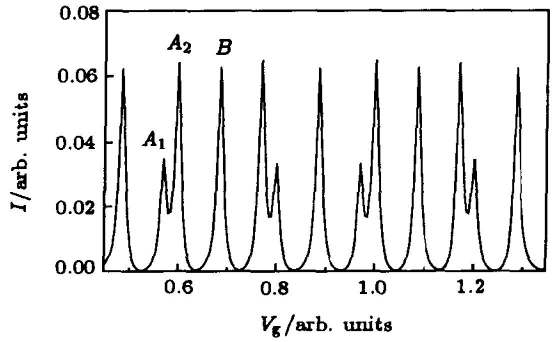

Fig.3. The current I vs the gate voltage V_g for $V < \Delta$. The QD has 10 states but with unequal level-spacing: $\Delta\epsilon_i = 0.17$ for even i, $\Delta\epsilon_i = 0.23$ for odd i, and $\epsilon_0 = 0$ at $V_g = 0$. The other parameters are the same as in Fig.1(c).

In the rest part of this paper, we will keep the assumption of equal level-spacing for simplicity.

B. The case with $V > \Delta$

In the case of $V > \Delta$, all kinds of the processes contribute to the current I, including Andreev reflection and all three kinds of the tunneling processes mentioned above, i.e., both I_A and I_1 are non-zero.

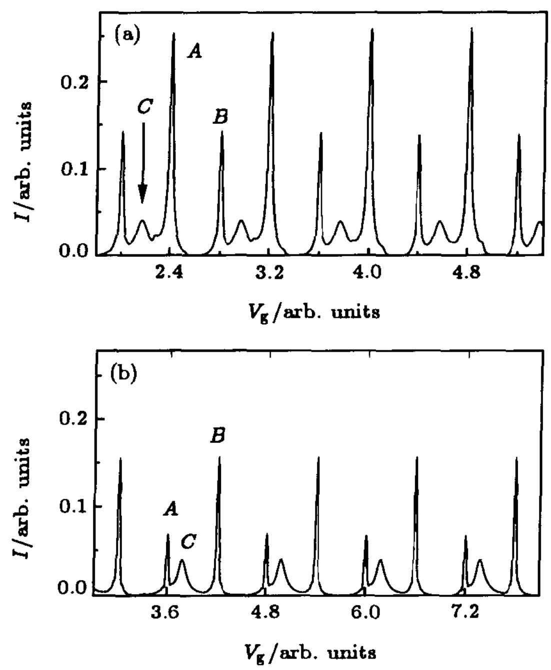

Fig.4. The current I vs the gate voltage V_g for $V > \Delta$. The QD has 10 states with equal level-spacing; and $\epsilon_0 = 0$ at $V_g = 0$. Other parameters are chosen as $\Gamma_L = \Gamma_R = 0.02$, $\Delta = 1$, and $V = 1.04$. (a) and (b) correspond to $\Delta\epsilon = 0.8$ and 1.2, respectively.

Here we studied I–V_g for V slightly larger than Δ (see Fig.4). The difference between Fig.4.(a) and (b) is due to the different level-spacing of the QD's states. Now three series of the peaks emerge in the curve, marked by "A", "B", and "C", respectively, and with the same intervals (or "periods") between the peaks for each series. The positions of the B-type peaks are in the middle of the A-type peaks; and the position of the C-type peak is shifted from the A-type peak by a certain amount which depends on the level-spacing $\Delta\epsilon$ and the gap Δ. The height of the C-type peak is the smallest one.

In the following calculation, we fix the parameters as indicated in Fig.4.(a), and set $\Delta\epsilon = 0.8$. Since $\epsilon_i = \epsilon_i^0 - V_g$ which varies with the gate voltage V_g, the state ϵ_4 is just below the chemical potential μ_L and above the gap Δ when $V_g = 2.2$ (see Fig.5(a)). So the conventional electron and quasi-particle tunneling processes are allowed, leading to the C-type peaks. With the increase of the gate voltage, each level of the QD moves downward. When $V_g = 2.4$, the state ϵ_3 is lined up with the chemical potential μ_R, and the energy difference between the state ϵ_4 or ϵ_2 and μ_R are equal (See Fig.5(b)). So the Andreev reflection can occur through either the state ϵ_3 itself or or other two states ϵ_4 and ϵ_2, leading to the A-type peaks with the largest amplitude (See Fig.4(a)). As V_g is increased further at $V_g = 2.8$, the energy difference between the state ϵ_4 or state ϵ_3 and μ_R are equal (not shown here), and both of ϵ_3 and ϵ_4 are below the chemical potential of the left lead, μ_L. Then the Andreev reflection occurs through the states ϵ_4 and ϵ_3, corresponding to the B-type peaks. For the case with symmetric barriers (as assumed in our calculations), i.e. $\Gamma_L = \Gamma_R$, the maximum probability of the Andreev reflection can reach one, but the conventional transmission probability is less than one because $\Gamma_L \neq \Gamma_R\tilde{\rho}_R$. Therefore the height of the C-type peak is the smallest one.

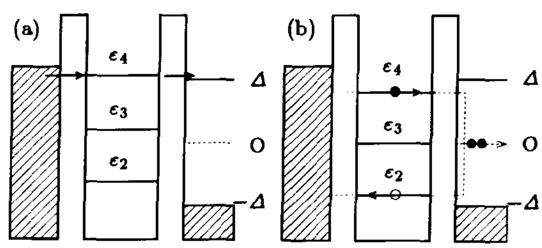

Fig.5. A schematic diagram for the tunneling processes responsible for the C-type and the A-type peaks. (a) and (b) describe the positions of the QD's states, and show the related conventional tunneling(C-type) and the Andreev tunneling(A-type) processes, respectively.